PETISCO is a novel protein complex required for 21U RNA biogenesis and embryonic viability

Ricardo J. Cordeiro Rodrigues[1], António Miguel de Jesus Domingues[1], Svenja Hellmann[1], Sabrina Dietz[2], Bruno F. M. de Albuquerque[1,3], Christian Renz[4], Helle D. Ulrich[4], Falk Butter[2], René F. Ketting[1]

Institute of Molecular Biology (IMB), Ackermannweg 4, 55128, Mainz, Germany

[1] IMB, Biology of Non-coding RNA Group

[2] IMB, Quantitative Proteomics Group

[3]Graduate Program in Areas of Basic and Applied Biology, University of Porto, 4099-003 Porto, Portugal.

[4]IMB, Maintenance of Genome Stability Group

correspondence: r.ketting@imb.de

ORCID Ketting: 0000-0001-6161-5621

ORCID Rodrigues: 0000-0002-0541-2229

ORCID Domingues: 0000-0002-1803-1863

ORCID Renz: 0000-0003-3164-3597

ORCID Ulrich: 0000-0003-0431-2223

Abstract

Piwi proteins are important for germ cell development in almost all animals studied thus far. These proteins are guided to specific targets, such as transposable elements, by small guide RNAs, often referred to as piRNAs, or 21U RNAs in *C. elegans*. In this organism, even though genetic screens have uncovered a number of potential 21U RNA biogenesis factors, little is known about how these factors interact or what they do. Based on the previously identified 21U biogenesis factor PID-1, we here define a novel protein complex, PETISCO, that is required for 21U RNA biogenesis. PETISCO contains both potential 5'-cap and 5'-phosphate RNA binding domains, suggesting involvement in 5' end processing. We define the interaction architecture of PETISCO and reveal a second function for PETISCO in embryonic development. This essential function of PETISCO is not mediated by PID-1, but by TOST-1. Vice versa, TOST-1 is not involved in 21U RNA biogenesis. Both PID-1 and TOST-1 are small, intrinsically disordered proteins that interact directly with the PETISCO protein ERH-2 (enhancer of rudimentary homolog 2) using a conserved sequence motif. Finally, our data suggest an important role for TOST-1:PETISCO in SL1 homeostasis in the early embryo. Our work describes the first molecular platform for 21U RNA production in *C. elegans*, and strengthens the view that 21U RNA biogenesis is built upon a much more widely used, snRNA-related pathway.

40 **Introduction**

41 Germ cells in many organisms depend critically on the integrity of a small RNA-driven
42 pathway known as the piRNA pathway [1 2]. This pathway is characterized by members of the
43 Piwi protein family that, bound to their small RNA cofactors (piRNAs), act in gene-regulatory
44 and transposon silencing pathways [3,4]. In the absence of these pathways, germ cells do not
45 form properly, ultimately leading to sterility. Even though this type of pathway is found in
46 the germ cells of most, if not all animals, the mechanistic details of the Piwi pathways are
47 remarkably different. In flies, for example, a piRNA amplification loop, driven by two Piwi
48 paralogs, is coupled to the activity of a third, nuclear Piwi protein that drives transcriptional
49 silencing [5 4]. In other animals, such as the silk moth, the nuclear branch seems to be absent,
50 while the Piwi amplification loop is present [6], and in mice a linear Piwi pathway drives
51 nuclear accumulation of a Piwi protein [4]. While transposons represent major targets for
52 these pathways, it is also clear that non-transposon targets are functionally relevant for
53 these pathways [7].

54

55 In *C. elegans*, the main Piwi protein is named PRG-1 (piwi related gene 1) and the small RNA
56 co-factors bound by PRG-1 are known as 21U RNAs [8-10]. This name stems from the fact that
57 these small RNAs are 21 nucleotides long, and have a strong bias for a 5' uracil. Target RNA
58 recognition by PRG-1:21U complexes does not depend on full-length base-pairing between
59 the 21U RNA and the target RNA [11,12], and results in the recruitment of RNA-dependent RNA
60 polymerase activity, that drives the synthesis of so called 22G RNAs [8,9]. These 22G RNAs,
61 named after their predominant 22 nucleotide length and 5' G bias, are bound by argonaute
62 proteins that are specific for nematodes (also referred to as WAGO-proteins), that ultimately
63 drive the silencing of the 21U target.

64

65 In absence of PRG-1, the germline deteriorates over generations, eventually leading to
66 sterility [13]. The defects that accumulate are most likely not genetic in nature, since the
67 phenotype can be reverted by, for instance, starvation [13]. These observations have led to the
68 suggestion that in *prg-1* mutants a form of stress accumulates and ultimately leads to germ
69 cell dysfunction [14]. More acute fertility defects can be observed in *prg-1* mutants when the
70 22G RNA biogenesis machinery is reactivated in zygotes, after being defective in both of the
71 parents. In this case, maternally provided PRG-1:21U complexes are required to prevent

immediate sterility, by preventing accumulation of 22G RNA populations that inappropriately silence genes that should be expressed [15,16]. This demonstrates that PRG-1, and its bound 21U RNA, has a critical function in maintaining a properly tuned 22G RNA population in the germ cells. Nevertheless, the impact of PRG-1 on transposon silencing is rather modest, as in *prg-1* mutants only activation of the Tc3 transposon has thus far been demonstrated [8].

Interestingly, the silencing of a 21U target, at least a transgenic one, can become independent of 21U RNAs themselves [5,17,18]. In this state, which has been named RNAe (for RNAi induced epigenetic silencing), the silencing has been completely taken over by a self-sustaining 22G RNA response. This includes a nuclear component that changes the histone methylation status of the targeted transgene, driven by the nuclear Argonaute protein HRDE-1 [5,17-19]. Possibly, such an RNAe state may explain why transposons are not more broadly upregulated in *prg-1* mutants, because in *prg-1;hrde-1* double mutants the Tc1 transposon is strongly activated [15]. How exactly RNAe is established is not clear, but once it is, it can be extremely stable, for over tens or more of generations [5,17,18].

Given the important function of 21U RNAs driving a potentially very powerful silencing response, the biogenesis of 21U RNAs is a critical process for the germ cells of *C. elegans*. Nevertheless, very little is known about the mechanistic steps of this process. The large majority of genes encoding 21U RNAs are found in two main clusters on chromosome IV, and are characterized by a very specific sequence motif in their promoter that defines the 5' end of the mature 21U RNA [20]. Transcription of these genes requires a protein named PRDE-1 and the transcription factor SNPC-4 [21,22], the latter of which is also known to be involved in transcription of other short structural RNAs, such as snRNAs and splice-leader RNAs [21]. An evolutionary analysis of 21U RNA loci in diverse nematodes has revealed that 21U loci may have evolved from snRNA loci [23]. These loci include both the strongly conserved U1, U2 loci, as well as loci producing so-called splice leader RNAs (SL1 and SL2), that are trans-spliced to the 5' ends of a large fraction of all mRNAs in *C. elegans* [24]. These observations raise the possibility that also other aspects of the 21U RNA pathway may have mechanistic links to snRNA biogenesis.

104 The 21U RNA precursor transcripts are short, around 27 nucleotides, and capped [25]. Even
105 though a biochemical reconstitution of the processing has not been achieved thus far, the
106 available data suggest the following order of steps in the maturation of the 21U precursor
107 transcripts into mature 21U RNAs [20,22,25-27]. First, the precursors are most likely processed at
108 the 5' end, resulting in de-capping and removal of two nucleotides. The enzymes involved
109 have not yet been identified, and whether this reaction is mediated by endo- or exo-
110 nucleolytic activities is not clear. This step is likely followed by loading of the 5'processed
111 precursor into PRG-1 and trimming of the 3' end by the 3'-5' exonuclease PARN-1 [28]. Finally,
112 the 3' end is 2'-O-methylated by HENN-1 [29-31]. Not much is known about other proteins
113 acting at these 21U maturation steps, even though a number of genes have been implicated
114 in this process [21,22,26,27 32].
115
116 Here, we follow up on our previous identification of PID-1 (piRNA induced silencing defective
117 1) as a protein essential for 21U RNA production [26]. Mutants lacking PID-1 produce very low
118 amounts of mature 21U RNAs, and the 21U-related molecules that remain tend to be
119 precursor transcripts, suggesting PID-1 acts at some step in 21U precursor processing. Other
120 factors potentially acting at this step of 21U biogenesis, TOFU-1, 2, 6 and 7, were identified
121 in a genome-wide RNAi screen [27]. How these factors interconnect, however, remained
122 unclear. We find, using immuno-precipitation (IP) and label free quantitative mass
123 spectrometry (IP-MS), that PID-1 interacts with two proteins that were identified in a
124 genome-wide RNAi screen for 21U RNA biogenesis factors: TOFU-6 and the unnamed protein
125 Y23H5A.3, henceforth referred to as PID-3. In addition, we identify two strongly conserved
126 proteins interacting with PID-1: IFE-3, a *C. elegans* eIF4E homolog, and ERH-2, one of the *C.*
127 *elegans* homologs of 'enhancer of rudimentary'. Enhancer-of-rudimentary homologs are
128 evolutionary very well conserved proteins, with homologs being present from plants to man.
129 Its mechanistic role is not very well established, but in *Schizosaccharomyces pombe* ERH1
130 drives the decay of meiotic transcripts, and interacts with the nuclear exosome and the
131 nuclear CCR4-NOT complex [33]. Since we always find PID-3, ERH-2, TOFU-6 and IFE-3 together
132 in a complex we named it PETISCO, for PID-3, ERH-2, TOFU-6, IFE-3 small RNA Complex. All
133 PETISCO proteins are required for 21U biogenesis. Additionally, PETISCO mutants display a
134 maternal effect lethal (Mel) phenotype, whereas *pid-1* and *prg-1* mutants are viable. We find
135 that this is caused by the fact that besides binding to PID-1, PETISCO can bind a protein with

136 similarities to PID-1. We named this protein TOST-1, for Twenty-One U pathway antagonist.
137 Mutants for *tost-1* produce 21U RNAs, display enhanced 21U-driven silencing and have a
138 Mel phenotype. PID-1 and TOST-1 both interact with ERH-2 using a conserved motif, strongly
139 suggesting a mutually exclusive mode of binding to PETISCO, where PID-1 implicates it in
140 21U RNA biogenesis and TOST-1 in another pathway that is essential for embryonic viability.
141 Our data suggest that this pathway may be involved in providing the embryo with resources
142 required for trans-splicing, especially with the SL1 splice leader RNA.
143
144 With these findings, we pave the way for a better understanding of how 21U precursor
145 transcripts are processed. The identification of PETISCO, plus its implication in at least two
146 distinct processes provides the new insight that 21U RNA processing is closely related to a
147 more widely conserved process: that of snRNP biogenesis. Combined with the fact that 21U
148 RNA transcription also bears strong signatures of an snRNA-history, an image arises in which
149 the 21U RNA pathway may have evolved out of an already existing small non-coding RNA
150 network that became linked to an Argonaute-driven gene-silencing program.

151 **Results**

152 **Identification of PID-1 interactors**

153 To identify proteins interacting with the 21U biogenesis factor PID-1 [26] we performed IPs
154 with PID-1 specific antibodies, followed by protein identification using mass spectrometry
155 (IP-MS). As control, we precipitated PID-1 from two independent *pid-1* loss of function
156 strains. Both experiments identified a rather restricted set of proteins (Figure 1a, S1a).
157 TOFU-6 and PID-3 were identified as the most prominent PID-1 interactors, and for the latter
158 we further validated the interaction with PID-1 through IP-Western blotting (Figure S1b).
159 Given that these two proteins were identified in an RNAi-screen for 21U biogenesis factors
160 [27], we considered these as functionally relevant PID-1 interactors. TOFU-6 is a protein with a
161 Tudor domain, a potential eIF4E interaction motif and an RRM domain, whereas PID-3 has an
162 RRM domain and a MID-domain (Figure S1c). Two other proteins were consistently
163 identified as PID-1 interactors: IFE-3 and ERH-2 (Figure 1a, S1a). IFE-3 is one of the five *C.*
164 *elegans* homologs of eIF4E. Previous work demonstrated that IFE-3 binds to the 7-
165 methylguanylate (m7G) Cap [34]. Interestingly, 21U precursor transcripts appear to be not
166 trans-spliced [25], implying that they have a m7G Cap structure at their 5' end. Hence, IFE-3
167 may bind to the 5' cap structure of the 21U precursor transcripts. ERH-2 is one of the two *C.*
168 *elegans* homologs of a protein known as 'enhancer of rudimentary'. Homologs of this
169 protein are strongly conserved from plants to mammals. Even though a protein structure for
170 the human homolog has been described [35], its molecular function is still unclear. In Figure
171 S1c we present a schematic of all these PID-1 interactors, with their identified domains.

172

173 We next probed the subcellular localization of PID-1 and its four identified interactors, by
174 expressing them from transgenes generated through the so-called miniMos approach (see
175 methods) [36]. For each gene we used its own promoter and 3' UTR sequences. All transgenes
176 were able to rescue mutant phenotypes (not shown) indicating the expressed proteins are
177 functional. All four interactors show a characteristic perinuclear, punctate localization in the
178 germline syncytium, overlapping partially, but not fully with the P-granule marker PGL-1
179 (Figure 1b,c). IFE-3 has a clear granular expression in the primordial germ cells in the embryo
180 (Figure S2b), whereas the remaining interactors show a dispersed cytoplasmic distribution
181 across the entire early embryo (Figure S2c). These results show that all the identified PID-1

182 interactors are expressed concomitantly in early embryos, and in the germline, where they
183 are found in close proximity to P-granules.
184
185 **PID-1 interactors mutually interact to form PETISCO**
186 To probe to what extent the identified PID-1 interactors reciprocally interact, and to what
187 extent they in turn interact with additional proteins, we performed IP-MS on TOFU-6, IFE-3,
188 PID-3 and ERH-2 in young adult animals, using the tagged proteins expressed from the
189 above-described transgenes. Extracts from non-transgenic wild-type animals were used as
190 negative controls. As shown in Figure 2a-d, these experiments revealed that all four proteins
191 co-precipitate with each other. In addition, we also found an uncharacterised protein
192 (C35D10.13) which systematically co-precipitated with the PID-1 interactors, but was absent
193 from the PID-1 IPs. This factor, which we named TOST-1, will be further described below.
194 These interactions are RNAse resistant. RNase treatment did not disrupt PID-3 interactions
195 (Figure S3a), and had very little effect on IFE-3 partners, resulting only in the loss of PID-1
196 (Figure S3b). We summarize the network of PID-1 interactors in Figure 2e. Given the strong
197 reciprocal interactions between these proteins, it is likely that they form a discrete complex.
198 We named this complex PETISCO, for PID-3, ERH-2, TOFU-6, IFE-3 small RNA Complex.
199
200 As mentioned before, IFE-3 is one of the *C. elegans* eIF4E homologs. Surprisingly, in our
201 experiments we do not detect any of the known translation initiation factors to be
202 associated with IFE-3. The transgenically expressed IFE-3 does rescue the *ife-3* mutant
203 phenotype (not shown), implying that IFE-3 may not play a role in initiating translation. We
204 do detect a number of additional proteins bound to IFE-3 which provide clues to IFE-3
205 function. One such protein is IFET-1, a homolog of human EIF4E nuclear import factor 1 and
206 a negative regulator of translation [37]. We further consistently detect many, if not all
207 components of the SMN complex [38]. The SMN complex plays a major role in snRNP
208 biogenesis, implicating IFE-3 in this process as well.
209
210 **PETISCO architecture**
211 Having established the components of PETISCO, we next dissected the molecular
212 interactions within this complex. Using the yeast-two-hybrid (Y2H) system we scored
213 interactions between each possible pair of individual PETISCO subunits (Figure 3a, S4a). This

214 resulted in the following interactions that are most likely to be direct: IFE-3 interacts only
215 with TOFU-6. TOFU-6 in turn interacts with PID-3, which in turn also interacts with ERH-2.
216 Finally, PID-1 and TOST-1 were both found to interact only with ERH-2. Self-interaction was
217 detected for ERH-2, though under lower stringency conditions, indicating that ERH-2 may be
218 present as a dimer in PETISCO.
219
220 We also investigated which domains of the PETISCO subunits are responsible for the protein
221 interactions using the same Y2H set-up. The putative eIF4E interaction motif [39 40] within the
222 C-terminus of TOFU-6 indeed is responsible for the interaction between TOFU-6 and IFE-3
223 (Figure 3b). No interactions were found for the Tudor domain of TOFU-6. The RRM domain
224 of TOFU-6 was found to bind to the RRM-domain of PID-3 (Figure 3c), and the same RRM
225 domain of PID-3 was found to also interact with ERH-2 (Figure 3d). Lower stringency and
226 control selections of the same experiments are shown in Figures S4b-d). This Y2H set-up did
227 not allow us to determine if the PID-3 RRM domain can sustain both the TOFU-6 and the
228 ERH-2 interaction simultaneously, however the fact that we find PID-3, TOFU-6 and ERH-2
229 strongly enriched in the IPs of one another, suggests that it can.
230
231 **PETISCO subunits are required for 21U RNA biogenesis and are essential for**
232 **embryogenesis**
233 Since at least two components of PETISCO, PID-1 and TOFU-6, play a major role in 21U RNA
234 biogenesis, we hypothesized that the other components are also part of this pathway. We
235 first tested whether they affect the silencing of a GFP sensor construct that reports on the
236 activity of the 21U pathway (21U sensor) [11]. We used a strain that contains this sensor plus a
237 *pid-1(xf14)* mutation that is rescued by transgenic expression of PID-1. In this strain, the
238 sensor is silenced (Figure 4a,b), although not completely. This partial 21U sensor-silencing
239 brings two advantages: first, the 21U sensor is not in an RNAe-state, in which it would no
240 longer be activated by loss of 21U RNAs; second, a semi-silenced state allows for scoring of
241 both increased and decreased sensor activity.
242
243 Animals from this sensitized sensor strain were subjected to RNAi targeting the various
244 PETISCO subunits and sensor activity was evaluated by microscopy and RT-qPCR (Figure
245 4a,b). As expected, RNAi against *pid-1* activated the sensor. Likewise, RNAi against *ife-3*, *pid-*

246 *3*, *tofu-6* and *erh-2* activated the sensor. These data show that PETISCO subunits, like the
247 PETISCO interactor PID-1, are required for a fully functional 21U RNA silencing pathway.
248
249 To extend the above observation to the overall 21U RNA population, we aimed to sequence
250 small RNAs from genetic mutants. For this, we created mutant alleles using CRISPR-Cas9 for
251 each of the PETISCO subunit genes. We were able to derive deletion alleles for *pid-3*, *erh-2*
252 and *ife-3* (Figure S5a), and isolated and sequenced small RNAs. We did not make mutants for
253 *tofu-6*, since RNAi on *tofu-6* was already shown to significantly reduce 21U RNA production
254 [27]. All experiments were done in triplicates. The results show that all tested PETISCO
255 subunits significantly affect 21U RNA biogenesis (Figure 4c). In particular, *pid-3(tm2417)* and
256 *erh-2(xf168)* mutants display a strong reduction in 21U RNA levels. The effect of *ife-3(xf102)*
257 mutation on 21U RNA accumulation is less pronounced, but still significant. Redundancy
258 between IFE-3 and other eIF4E homologs, could be a reason for this less pronounced effect
259 on 21U RNA levels, as we find IFE-1, a non-selective TMG/m7G binder [34], enriched in some of
260 our IP-MS experiments (Figure 2a-c, S3b). Other types of small RNAs, such as 22G, 26G and
261 miRNAs were mostly not affected by the tested mutations (Figure 4c and S5b-d). We note
262 that so-called type II 21U RNAs, which come from loci lacking the canonical Ruby motif and
263 are expressed at much lower levels [25], are only mildly, or not at all affected by loss of
264 PETISCO components.
265
266 Besides the defects in 21U biogenesis, the mutant alleles also display a so-called maternal
267 effect lethal (Mel) phenotype: homozygous mutant offspring from a heterozygous animal
268 develop into fertile adults, but the embryos display a fully penetrant arrest and never hatch
269 (Table 1). This phenotype has already been described for *tofu-6*, which is also known as *mel-*
270 *47* [41]. The *ife-3* mutant displays a mixed phenotype, as previously described [42]: homozygous
271 mutant offspring from a heterozygous animal develop into adults that can either display a
272 masculinized germline (Mog) or a Mel phenotype. Interestingly, we note that *pid-1* mutants
273 also display a Mog phenotype, albeit at low frequency (Table 1 and Figure S6).
274
275 **PID-1 and TOST-1 define distinct functions of PETISCO**
276 The fact that PETISCO genes are essential for embryogenesis contrasts with the fact that loss
277 of 21U RNAs through other means, such as loss of PRG-1 or PID-1, does not result in a Mel

278 phenotype. Interestingly, RNAi-knockdown of *tost-1* resulted in an embryonic lethal
279 phenotype (not shown). In our IP-MS experiments, we consistently found this protein to
280 interact with the PETISCO subunits (Figure 2a-d), yet not with PID-1 (Figure 1a and S1a).
281 Furthermore, *tost-1(rnai)* displays enhanced, rather than disrupted silencing of the
282 sensitized 21U sensor (Figure 4a,b). This phenotype lead us to name this protein TOST-1,
283 short for twenty-one U antagonist.
284
285 We tested both PID-1 and TOST-1 for interactions with PETISCO subunits. We found that
286 both PID-1 and TOST-1 specifically interact only with ERH-2 (Figure 3a). While the overall
287 amino-acid sequences of PID-1 and TOST-1 do not display convincing homology (Figure S7a),
288 when aligned with PID-1 and TOST-1 homologs from other nematode species, a conserved
289 motif emerges ($_{[+][+]\Psi(T/S)}$**L**$_{(N/S)[-]}$**RF**$_{x\Psi xxx}$**G**$_{(Y/F)}$ – Figure 5a). Strikingly, the *xf14* allele we
290 identified for *pid-1* in our previously described genetic screen caries a mutation of the fully
291 conserved arginine residue within this motif (R61C) [26]. When introduced into the Y2H
292 experiment, PID-1(R61C) did not interact with ERH-2, and the analogous mutation in TOST-1
293 also disrupted its ERH-2 interaction (Figure 5b). These data strongly suggest that both PID-1
294 and TOST-1 share a conserved short motif required for ERH-2 interaction.
295
296 To further understand TOST-1 function we generated loss of function alleles for *tost-1* using
297 CRISPR-Cas9 (Figure S5a). Loss of TOST-1 did not significantly affect 21U RNA biogenesis
298 (Figure 5c, S7b), but did result in a fully penetrant Mel phenotype (Table 1). Among the
299 alleles we generated, we found one allele, *tost-1(xf196)*, with a 58bp deletion which
300 removes the splice acceptor site of its third exon (Figure S5a), resulting in either a frame-
301 shift or a C-terminal truncation. *tost-1(xf196)* displays a temperature-sensitive (TS) effect: at
302 25°C the animals are fully Mel, while at 15°C the animals are viable. The fact that this allele
303 appears to be mostly functional at 15°C suggests that the N-terminal part of TOST-1 is the
304 critical part of this protein. The interaction motif we identified is still intact in *tost-1(xf196),*
305 consistent with the idea that it is essential for TOST-1 function. This TS allele allowed us to
306 probe the Mel phenotype in more detail, through temperature-shift experiments (Figure
307 S7c). First, animals grown at the restrictive temperature were able to produce viable
308 offspring after shifting them to the permissive temperature. This shows that there are no
309 structural or developmental defects in the germline of these animals that prevent them from

310 producing live offspring. Second, the TS allele allows us to probe when TOST-1 function is
311 required. The time required for animals shifted to the permissive temperature to produce
312 viable embryos (8 hours) is significantly longer than the time it takes from fertilization to
313 egg-laying (approximately 200 min at 15°C), implying that the embryos laid after 8 hours
314 were fertilized and raised at the permissive temperature. Yet, they are still arresting. This
315 observation places TOST-1 activity within the gonad. However, when animals are shifted
316 from permissive to restrictive temperature, the first arrested embryos are laid already after
317 two hours. This is very close to the time of residency within the uterus (approximately 150
318 min 25°C), and hence these embryos had been fertilized very close to the time of the
319 temperature shift, in a gonad that was still functional. This suggests TOST-1 also has a
320 function within the embryo. This is consistent with PETISCO subunit expression within early
321 embryos (Figure S2c).
322
323 In conclusion, our data shows that both TOST-1 and PID-1 bind to the same PETISCO subunit,
324 while loss of these two proteins results in different phenotypes. The combined phenotypes
325 of both *pid-1* and *tost-1* mutants is found in mutants for the other PETISCO subunits,
326 strongly suggesting that PID-1 and TOST-1 define two distinct aspects of PETISCO function.
327
328 **PETISCO interacts with SL1 RNA**
329 Given the known links between the 21U RNA pathway and snRNA transcription, the fact that
330 we find many SMN-complex components in IFE-3 IPs, and that at least one SMN component
331 has a Mel phenotype (MEL-46), we hypothesized that the essential function of PETISCO is
332 linked to snRNA homeostasis. Consistent with this idea, we noticed a striking accumulation
333 of a 3' fragment of SL1 RNA in a number of the mutants we tested (Figure 6a,b, S8a). Such
334 accumulation was less pronounced, or absent for another small non-coding RNA that is
335 produced from the same gene cluster as SL1, 5S rRNA (Figure 6b,c). Importantly, this
336 enrichment of SL1 fragments was very clear in *tost-1* mutants, but absent in *pid-1* mutants.
337 Also *ife-3* mutants and *erh-2* mutants displayed a similar accumulation in all the replicates
338 that we sequenced. Mutants for *pid-3*, however, did not show the accumulation (Figure 6b).
339 For SL2 we only observe the enrichment in *ife-3* mutant libraries (Figure S8b), but we point
340 out that SL2 read counts are comparatively very low.
341

342 To further test a potential link between PETISCO and SL1 RNA, we probed whether SL1, or
343 SL1 fragments may be bound by PETISCO. To test this, we performed RIPseq experiments on
344 IFE-3 and PID-3. We performed these experiments in quadruplicate, and also performed
345 triplicate mock IPs from wild-type animals. Since full SL1 transcripts, but also 21U precursors
346 are capped, we treated the RNA with RppH to remove 5' caps before cloning. We detect
347 strong and significant enrichment of SL1, and to a lesser extent SL2 sequences in both PID-3
348 and IFE-3 IPs (Figure 6c, S8c). In contrast, transcripts from 21U loci, 5S rRNA and snRNAs are
349 not enriched, or are even depleted (Figure 6c, S8c). The read coverage over the SL1
350 transcript shows that two fragments are detected: one at the 5' and another at the 3' end
351 (Figure 6d, S8d). The 5' fragment is capped, as this fragment is absent from libraries from
352 non-RppH treated RNA (Figure 6d). We conclude that PETISCO binds to SL1 RNA and that loss
353 of PETISCO leads to an accumulation of SL1 RNA fragments.

354 **Discussion**

355 We have identified a protein complex, named PETISCO, that is involved in at least two
356 different pathways. PID-1 guides PETISCO towards 21U RNA biogenesis, whereas TOST-1
357 brings PETISCO to a pathway that is essential for embryogenesis, but does not involve 21U
358 RNAs. Here we discuss various aspects of this complex and present hypotheses for the
359 different potential functions of PETISCO.

360

361 **PID-3 and TOFU-6 define the core of PETISCO**

362 Judging by the enrichments found in all IPs and the similarities in phenotypes of the
363 corresponding mutants it seems likely that two proteins, PID-3 and TOFU-6 form the core of
364 the PETISCO complex, and that the other identified factors may add as adaptors for specific
365 functions of PETISCO. What could the core function(s) of this complex be? Based on protein
366 identities and obtained results we consider the following, non-exclusive possibilities.

367

368 Based on the presence of two RRM domains, one in TOFU-6 and one in PID-3, this complex
369 likely has RNA binding activities. Indeed, our RIPseq experiment identified 3' fragments of
370 SL1 and SL2 bound to PETISCO. Interestingly, we found that both RRM domains act as
371 protein-protein interaction modules. This does not mean that these two RRM domains
372 cannot also be involved in RNA binding, as combined RNA- and protein-binding activities for
373 RRM domains have been described before [43]. Possibly, the assembly of the RRM-RRM
374 contact between PID-3 and TOFU-6 is facilitated by RNA. Even though we find that RNase
375 treatment does not affect the pull-down efficiency between PID-3 and TOFU-6, the RNA
376 involved may be inaccessible to RNases.

377

378 In addition to the RRM motifs, the MID-domain present in PID-3 also brings potential for
379 protein-RNA-interactions. The MID-domain has thus far been described in context of
380 argonaute proteins where it mediates interactions with the 5' end of the bound small RNA
381 co-factor [44]. It is curious to find such a domain in a protein involved in generating small RNA
382 co-factors for an argonaute protein. We hypothesize that the MID domain of PID-3 may help
383 to stabilize a 5' processing intermediate. This would imply PETISCO as a 5'end processing
384 platform for 21U RNAs. Biochemical reconstitution experiments will be required to test this.

385

386 The Tudor domain of TOFU-6 likely represents a protein-protein interaction unit. Tudor
387 domains are known to interact with methylated arginines, and within perinuclear granules,
388 where PETISCO is found, such methylated arginines are likely abundant [45]. Hence, the Tudor
389 domain may be involved in sequestering PETISCO to these granules, possibly to PRG-1. PRG-
390 1 itself has an N-terminal protein sequence that is highly suggestive of arginine methylation.
391 In one of our IFE-3 pull-downs, we do enrich for PRG-1 (Figure 2a), supporting this possibility.
392
393 **ERH-2: Bridge between core-PETISCO and PETISCO-guiding factors?**
394 The presence of ERH-2 provides hints for PETISCO function. In *S. pombe*, Erh1 forms a tight
395 complex with a protein named Mmi and together they are involved in nuclear mRNA
396 degradation of meiotic transcripts, involving proteins such as ARS2 and the CCR4-NOT
397 complex [33]. Hence, Erh1 in *S. pombe* appears to act as a bridge between an RNA binding
398 protein (Mmi) and an RNA processing machinery. Our data strongly suggest that ERH-2 in *C.*
399 *elegans* has a very similar function. On the one hand, it binds core PETISCO and on the other
400 hand either PID-1 or TOST-1, which set the function of the complex (see below).
401
402 ERH-related proteins in other systems, including *S. pombe* and human cells, are nuclear
403 proteins [33], while we find ERH-2 to be present mainly in perinuclear granules. Related to this
404 it is interesting to note that *C. elegans* has a second ERH-like protein T21C9.4. Alignments
405 show that this homolog is more closely related to *S. pombe* and human ERH1 (not shown),
406 raising the possibility that T21C9.4 in *C. elegans* is nuclear and may be coupled to nuclear
407 RNA processing.
408
409 **Bi-functionalization of PETISCO through PID-1 and TOST-1**
410 We show that PETISCO has at least two functions: 21U RNA biogenesis and another,
411 essential function in embryogenesis, which is likely related to SL1/2 snRNP homeostasis.
412 These two functions can be functionally separated through two different 'adapter'-proteins
413 (PID-1 and TOST-1) that bind to PETISCO via ERH-2. The overall homology between PID-1 and
414 TOST-1 is very low. Nevertheless, we identified a motif that is required for binding to ERH-2.
415 Hence, both proteins likely bind to PETISCO in a mutually exclusive way. Indeed, no TOST-1
416 was detected in PID-1 IPs, and Zeng et al. (accompanying manuscript) did not find PID-1 in
417 their TOST-1 IPs. An IP-MS experiment on PID-3 in absence of PID-1 (therefore enriching for

418 TOST-1:PETISCO) did not reveal much change compared to wild-type (not shown), suggesting
419 that stable interactions within PID-1:PETISCO and TOST-1:PETISCO are very similar and do
420 not provide further insights into the differential activities of PID-1 and TOST-1.
421
422 **Potential roles for IFE-3**
423 IFE-3 has been shown to bind m7G Cap structures, and to bind much less efficiently to the
424 typical TMG Cap structures found on the majority of trans-spliced mRNAs in *C. elegans* [34].
425 This activity of IFE-3 makes it a good candidate for binding 21U RNA precursors at a stage
426 before 5' processing. IFE-3 IP-MS experiments also enrich mildly for proteins involved in de-
427 capping (e.g. EDC-3, CAR-1, CGH-1 – Figure 2a). In relation to 21U RNA biogenesis, it is an
428 intriguing option that IFE-3 binds 21U precursor transcripts through their 5' cap structure,
429 after which they become de-capped by associated de-capping activities. IFE-3, however, is
430 not essential for 21U generation. This could be due to either functional redundancy with IFE-
431 1, which we regularly detect in our IP-MS experiments. Alternatively, IFE-3 has no direct role
432 in 21U RNA processing, and the small drop of 21U levels in *ife-3* mutants is an indirect effect,
433 for instance through effects on PETISCO overall stability.
434
435 We find that IFE-3 consistently comes down with many, if not all proteins found in the so-
436 called SMN complex. This complex is well known for its involvement in snRNP assembly [38]. In
437 *C. elegans*, the SMN complex has also been shown to be required for SL1 trans-splicing [46].
438 We note that a homolog for Gemin5, which has been shown to bind the m7G Cap structure
439 of pre-mature snRNAs in human cells [47], is not encoded by the *C. elegans* genome. Given the
440 cap-binding activity of IFE-3 and its association with the other SMN complex subunits, IFE-3
441 may fulfil this function in *C. elegans*. We note that like loss of IFE-3 [42], loss of the *C. elegans*
442 Gemin3 homolog, named MEL-46 [41], and the U2 snRNP-associated factor MOG-2 [48] also
443 result in Maternal effect lethality (Mel) and Masculinization of the germline (Mog)
444 phenotypes, further strengthening the links between IFE-3 and snRNP homeostasis. Given
445 that the SMN-complex proteins are not found in the IPs of any of the other PETISCO
446 subunits, the IFE-3-SMN interaction is likely to be physically separated from PETISCO. Finally,
447 it is interesting to note that *pid-1* mutants, but not *tost-1* mutants, also display a Mog
448 phenotype, albeit at a low frequency. Considering the interplay between PID-1 and TOST-1,

449 this could relate from excessive, or ectopic TOST-1:PETISCO in *pid-1* mutants affecting the
450 IFE-3-SMN interplay.
451
452 **Potential mechanisms behind the Mel and 21U phenotypes of PETISCO mutants**
453 Our data clearly show that PETISCO has at least two functions. Its role in 21U RNA biogenesis
454 is non-essential and is guided by PID-1. A second function, which is essential for early
455 development, is linked to PETISCO via TOST-1. While our current data do not provide
456 mechanistic details on molecular PETISCO function, they do provide interesting leads as to
457 what the essential function of PETISCO may be.
458
459 As mentioned above, PETISCO contains proteins with domains that interact with the 5' ends
460 of RNA, either capped or phosphorylated, raising the possibility PID-1-bound PETISCO plays a
461 role in 5' end processing of 21U precursor transcripts. In our RIP experiments, we did not
462 detect 21U RNA precursor molecules, suggesting that either levels are too low to be
463 detected in a RIP experiment, or that their processing is too fast. Given that RIP experiments
464 typically have high backgrounds, this may easily prevent detection of significant
465 enrichments. In view of the phenotypes and protein domains within PETISCO, we consider it
466 very likely that PETISCO does interact with 21U RNA precursors.
467
468 But what could the molecular function of PID-1-bound PETISCO be? In absence of PETISCO
469 21U RNA levels drop strongly, but we note that so-called type II 21U RNA levels are much
470 less affected (Figure S5b). These 21U RNA species do not derive from loci with the typical
471 Ruby-motif, and are expressed at much lower levels than type I 21U RNAs. We hypothesize
472 that PETISCO may function to specifically stimulate the processing of pre-cursors that come
473 from Ruby-motif-containing 21U loci, such that the PRG-1 RNP pool is dominated by PRG-1
474 protein bound to type I 21U RNAs.
475
476 TOST-1-bound PETISCO may have a similar function, only then coupled to the production of
477 an RNP that is essential for early development. Our RIPseq and mutant small RNAseq data
478 indicate that this could involve the SL1 snRNP. Our interpretation of these data is that
479 PETISCO binds full-length SL1 transcripts, but that these are partially degraded by nucleases
480 during the RIP-procedure, or within the animals when further processing of the complex is

481 stalled due to loss of PETISCO subunits such as TOST-1 or IFE-3. But how would this explain
482 the maternal effect lethality phenotype of PETISCO mutants? SL1 is a generally required
483 splice-leader RNA, and mutants that carry a large deletion covering the SL1 loci display a
484 direct embryonic lethal phenotype [49]. If PETISCO would have a core function in trans-splicing
485 one would expect a similarly severe zygotic phenotype. We hypothesize that PETISCO
486 specifically helps the accumulation of a large pool of SL1 snRNPs that will be maternally
487 loaded into the embryos. Later in development, when the demand for SL1 snRNPs may have
488 dropped, PETISCO may therefore not be required. This would create an interesting parallel
489 to 21U RNPs, that are also provided maternally [15].
490
491 Clearly, additional studies will be required to resolve the molecular function of PETISCO in
492 21U RNA processing and further test its role in SL1 homeostasis during early development.
493 However, our data firmly show that PETISCO is a 21U biogenesis complex, and in addition
494 has an essential role during early development. Our work shows that the processing of 21U
495 RNAs is likely derived from a much more widely conserved mechanism, and provides a new
496 and exciting view into how small RNA biogenesis can be intertwined with other gene-
497 regulatory mechanisms.
498

499 **Figure Legends**
500
501 **Figure 1 – PID-1 interactors reside in P-Granules**
502 **a)** Volcano plot representing label-free proteomic quantification of PID-1 IPs from non-
503 gravid adult extracts. IPs were performed and analyzed in quadruplicates. The x-axis
504 represents the median fold enrichment of individual proteins in wild type (WT) versus
505 *pid-1(xf14)* mutant strain. y-axis indicates -Log_{10}(p-value) of observed enrichments.
506 Dashed lines represent thresholds at p=0.05 and 2-fold enrichment. Blue data points
507 represent values out of scale. Red and Green data points represent values above and
508 below threshold, respectively.
509 **b and c)** Expression pattern and localization of tagged PETISCO components and P-
510 granule marker PGL-1. Endogenous promotors and 3'UTRs were used for PETISCO
511 proteins. Proteins and observable tags indicated in the panels. **b)** Immunostaining
512 images acquired with laser scanning confocal microscope. **c)** Live worm images
513 acquired under wide field fluorescent microscope. Scale bars represent 5 µm.
514 Contrast of images has been enhanced.
515
516 **Figure 2 – PID-1 interactors form a novel protein complex, PETISCO**
517 **a-d)** Volcano plot representing label-free proteomic quantification of quadruplicate **a)**
518 3xFLAG::mCherry::IFE-3;*ife-3(xf101)*; **b)** PID-3::mCherry::Myc;*pid-3(tm2417)*; **c)** TOFU-
519 6::GFP::HA;*tofu-6(it20)* and **d)** ERH-2::GFP::OLLAS;*erh-2(xf168)* IPs from non-gravid
520 adult extracts. The x-axis represents the median fold enrichment of individual
521 proteins in control (WT) versus transgenic strain. y-axis indicates -Log_{10}(p-value) of
522 observed enrichments. Dashed lines represent thresholds at p=0.05 and 2-fold
523 enrichment. Blue data points represent values out of scale. Red and Green data
524 points represent above and below threshold respectively.
525 **e)** Venn Diagram summarizing significant interactions in PETISCO protein IPs.
526 *represents protein found significantly enriched in only one experiment of
527 3xFLAG::mCherry::IFE-3;*ife-3(xf101)* IP.
528
529 **Figure 3 – PETISCO Architecture**
530 **a-d)** Yeast two-hybrid interaction assays of PETISCO subunits in low ($TRP^-LEU^-HIS^-$) or high
531 stringency media ($TRP^-LEU^-HIS^-ADE^-$) as indicated. Interactions were screened in
532 both Y2H orientations. **a)** Full length proteins **b)** TOFU-6 and individual domains
533 tested for interaction with full length IFE-3 **c)** Interactions between PID-3 and TOFU-
534 6 **d)** Interaction between PID-3 and ERH-1. For details on domains and other
535 selection conditions see Figure S4.
536
537 **Figure 4 – PETISCO is required for 21U RNA biogenesis**
538 **a)** Wide field fluorescent microscopy of adult hermaphrodites carrying GFPH2B-21U
539 sensor transgene in a sensitized background. Worms were subjected to RNAi via
540 feeding (targets indicated in figure) from L1 larval stage to adulthood. Empty RNAi
541 Vector serves as negative control. Scale Bar 10 µm.
542 **b)** Quantitative RT-PCR of 21U sensor transgene in adult worm populations of A). Values
543 are obtained from experimental triplicates and technical duplicates, normalized to

544 *pmp-3* mRNA levels. Significance was tested with Student's t-test: **p-value<0.01;
545 *p-value<0.05. Error bars represent standard deviation.
546 **c)** Global level of type I 21U RNA and miRNAs in the indicated strains. Values are in
547 reads per million (RPM). Individual data points of three independent replicates are
548 shown and horizontal bar represents the mean. Significance was tested with
549 Student's t-test and p-values are indicated in the graph.
550
551 **Figure 5 – TOST-1 is essential but not required for 21U RNA biogenesis**
552 **a)** Alignment of a short region of PID-1 and TOST-1 homologs from different nematodes.
553 Conserved arginine residue was found to be mutated in *pid-1(xf14)* as indicated.
554 Consensus sequence is presented below alignment. Alignment performed with
555 MUSCLE v3.8 [50] and representation with ESPrit v3.0 [51].
556 **b)** Y2H interaction assay of PID-1, TOST-1 and PID-1/TOST-1 carrying the corresponding
557 arginine mutation found in pid-1(xf14). High stringency plates ($TRP^-LEU^-HIS^-ADE^-$)
558 were used in the presented figure. For other conditions please see Figure S4d.
559 **c)** Global levels of type I 21U RNA and miRNAs in wild type (N2), *pid-1(xf35)* and *tost-*
560 *1(xf194)* gravid adult worms. Values are in reads per million (RPM). Individual data
561 points of three independent replicates are shown and horizontal bar represents the
562 mean. Significance was tested with Student's t-test and p-values are indicated in the
563 graph.
564
565 **Figure 6 – PETISCO interacts with SL1 snRNA**
566 **a)** Schematic representation of the Splicing Leader 1 RNA.
567 **b)** Global levels of SL1 RNA and 5S rRNA in wild type (N2), *pid-1(xf35)* and *tost-1(xf194)*
568 gravid adult worms and *pid-3(tm2417), erh-2(xf168)* and *ife-3(xf102)* non-gravid
569 adults. Values are in reads per million (RPM). Individual data points of three
570 independent replicates are shown and horizontal bar represents the total mean.
571 Significance was tested with Student's t-test and p-values are indicated in the graph.
572 **c)** Fold enrichments of SL1 RNA and 5S rRNA in Mock (N2), 3xFLAG::mCherry::IFE-3;*ife-*
573 *3(xf101)*; and PID-3::mCherry::Myc;*pid-3(tm2417)* RIPs over paired inputs in non-
574 gravid adult worms. Top row displays non-treated and bottom row RppH treated
575 samples. Individual data points of three independent replicates are shown and
576 horizontal bar represents the mean. Significance was tested with Student's t-test and
577 p-values are indicated in the graph.
578 **d)** Coverage profile, normalized to paired input, of SL1, of the data displayed in **c**. Colors
579 under SL1 RNA correspond to scaled colors represented in **a.**
580
581 **Figure 7 – Schematic representation of PETISCO function**
582 A schematic of the proposed PETISCO activity, displaying its dual function. One in 21U
583 biogenesis and another potentially linking to splice leader homeostasis. The two different 5'
584 end binding domains may reflect stabilization of different RNA species, and may reflect 5'
585 end processing of transcripts bound by PETISCO. ERH-2 serves as an anchor for PID-1 or

586 TOST-1 driving PETISCO function towards 21U RNA biogenesis or SL1 homeostasis
587 respectively.
588
589 **Table 1 – PETISCO displays maternal effect lethality**
590 “n.a.” not applicable; “n.d.” not determined; “-“ mild 21U RNA defect; “--“ severe 21U RNA
591 defect; “+” no 21U RNA defect; “(TS)” temperature sensitive; “#” counts are for gonadal
592 arms (n=38) due to mixed phenotypes in individuals; “*” according to Goh *et al*. [27].
593

594 **References**

595 1. Ketting, R.F. The many faces of RNAi. *Dev Cell* **20**, 148-61 (2011).
596 2. Weick, E.M. & Miska, E.A. piRNAs: from biogenesis to function. *Development* **141**,
597 3458-71 (2014).
598 3. Luteijn, M.J. & Ketting, R.F. PIWI-interacting RNAs: from generation to
599 transgenerational epigenetics. *Nat Rev Genet* **14**, 523-34 (2013).
600 4. Czech, B. & Hannon, G.J. One Loop to Rule Them All: The Ping-Pong Cycle and piRNA-
601 Guided Silencing. *Trends Biochem Sci* **41**, 324-337 (2016).
602 5. Luteijn, M.J. et al. Extremely stable Piwi-induced gene silencing in Caenorhabditis
603 elegans. *EMBO J* **31**, 3422-30 (2012).
604 6. Sakakibara, K. & Siomi, M.C. The PIWI-Interacting RNA Molecular Pathway: Insights
605 From Cultured Silkworm Germline Cells. *Bioessays* **40**(2018).
606 7. Rojas-Rios, P. & Simonelig, M. piRNAs and PIWI proteins: regulators of gene
607 expression in development and stem cells. *Development* **145**(2018).
608 8. Das, P.P. et al. Piwi and piRNAs act upstream of an endogenous siRNA pathway to
609 suppress Tc3 transposon mobility in the Caenorhabditis elegans germline. *Mol Cell*
610 **31**, 79-90 (2008).
611 9. Batista, P.J. et al. PRG-1 and 21U-RNAs interact to form the piRNA complex required
612 for fertility in C. elegans. *Mol Cell* **31**, 67-78 (2008).
613 10. Wang, G. & Reinke, V. A C. elegans Piwi, PRG-1, regulates 21U-RNAs during
614 spermatogenesis. *Curr Biol* **18**, 861-7 (2008).
615 11. Bagijn, M.P. et al. Function, targets, and evolution of Caenorhabditis elegans piRNAs.
616 *Science* **337**, 574-578 (2012).
617 12. Lee, H.C. et al. C. elegans piRNAs mediate the genome-wide surveillance of germline
618 transcripts. *Cell* **150**, 78-87 (2012).
619 13. Simon, M. et al. Reduced insulin/IGF-1 signaling restores germ cell immortality to
620 Caenorhabditis elegans Piwi mutants. *Cell Rep* **7**, 762-73 (2014).
621 14. Heestand, B., Simon, M., Frenk, S., Titov, D. & Ahmed, S. Transgenerational Sterility of
622 Piwi Mutants Represents a Dynamic Form of Adult Reproductive Diapause. *Cell Rep*
623 **23**, 156-171 (2018).
624 15. de Albuquerque, B.F., Placentino, M. & Ketting, R.F. Maternal piRNAs Are Essential
625 for Germline Development following De Novo Establishment of Endo-siRNAs in
626 Caenorhabditis elegans. *Dev Cell* **34**, 448-56 (2015).
627 16. Phillips, C.M., Brown, K.C., Montgomery, B.E., Ruvkun, G. & Montgomery, T.A. piRNAs
628 and piRNA-Dependent siRNAs Protect Conserved and Essential C. elegans Genes from
629 Misrouting into the RNAi Pathway. *Dev Cell* **34**, 457-65 (2015).
630 17. Ashe, A. et al. piRNAs can trigger a multigenerational epigenetic memory in the
631 germline of C. elegans. *Cell* **150**, 88-99 (2012).
632 18. Shirayama, M. et al. piRNAs initiate an epigenetic memory of nonself RNA in the C.
633 elegans germline. *Cell* **150**, 65-77 (2012).
634 19. Buckley, B.A. et al. A nuclear Argonaute promotes multigenerational epigenetic
635 inheritance and germline immortality. *Nature* **489**, 447-51 (2012).
636 20. Ruby, J.G. et al. Large-scale sequencing reveals 21U-RNAs and additional microRNAs
637 and endogenous siRNAs in C. elegans. *Cell* **127**, 1193-207 (2006).
638 21. Kasper, D.M., Wang, G., Gardner, K.E., Johnstone, T.G. & Reinke, V. The C. elegans
639 SNAPc component SNPC-4 coats piRNA domains and is globally required for piRNA
640 abundance. *Dev Cell* **31**, 145-58 (2014).

641 22. Weick, E.M. et al. PRDE-1 is a nuclear factor essential for the biogenesis of Ruby
642 motif-dependent piRNAs in C. elegans. *Genes Dev* **28**, 783-96 (2014).
643 23. Beltran, T. et al. Evolutionary analysis im[licates RNA polymersase II pausing and
644 chromatin structure in nematode piRNA biogenesis. *BioRxiv*
645 https://doi.org/10.1101/281360 (2018).
646 24. Blumenthal, T. Trans-splicing and operons in C. elegans. *WormBook*, 1-11 (2012).
647 25. Gu, W. et al. CapSeq and CIP-TAP identify Pol II start sites and reveal capped small
648 RNAs as C. elegans piRNA precursors. *Cell* **151**, 1488-500 (2012).
649 26. de Albuquerque, B.F. et al. PID-1 is a novel factor that operates during 21U-RNA
650 biogenesis in Caenorhabditis elegans. *Genes Dev* **28**, 683-8 (2014).
651 27. Goh, W.S. et al. A genome-wide RNAi screen identifies factors required for distinct
652 stages of C. elegans piRNA biogenesis. *Genes Dev* **28**, 797-807 (2014).
653 28. Tang, W., Tu, S., Lee, H.C., Weng, Z. & Mello, C.C. The RNase PARN-1 Trims piRNA 3'
654 Ends to Promote Transcriptome Surveillance in C. elegans. *Cell* **164**, 974-84 (2016).
655 29. Kamminga, L.M. et al. Differential impact of the HEN1 homolog HENN-1 on 21U and
656 26G RNAs in the germline of Caenorhabditis elegans. *PLoS Genet* **8**, e1002702 (2012).
657 30. Billi, A.C. et al. The Caenorhabditis elegans HEN1 ortholog, HENN-1, methylates and
658 stabilizes select subclasses of germline small RNAs. *PLoS Genet* **8**, e1002617 (2012).
659 31. Montgomery, T.A. et al. PIWI associated siRNAs and piRNAs specifically require the
660 Caenorhabditis elegans HEN1 ortholog henn-1. *PLoS Genet* **8**, e1002616 (2012).
661 32. Cecere, G., Zheng, G.X., Mansisidor, A.R., Klymko, K.E. & Grishok, A. Promoters
662 recognized by forkhead proteins exist for individual 21U-RNAs. *Mol Cell* **47**, 734-45
663 (2012).
664 33. Sugiyama, T. et al. Enhancer of Rudimentary Cooperates with Conserved RNA-
665 Processing Factors to Promote Meiotic mRNA Decay and Facultative
666 Heterochromatin Assembly. *Mol Cell* **61**, 747-759 (2016).
667 34. Jankowska-Anyszka, M. et al. Multiple isoforms of eukaryotic protein synthesis
668 initiation factor 4E in Caenorhabditis elegans can distinguish between mono- and
669 trimethylated mRNA cap structures. *J Biol Chem* **273**, 10538-42 (1998).
670 35. Arai, R. et al. Crystal structure of an enhancer of rudimentary homolog (ERH) at 2.1
671 Angstroms resolution. *Protein Sci* **14**, 1888-93 (2005).
672 36. Frokjaer-Jensen, C. et al. Random and targeted transgene insertion in Caenorhabditis
673 elegans using a modified Mos1 transposon. *Nat Methods* **11**, 529-34 (2014).
674 37. Sengupta, M.S. et al. ifet-1 is a broad-scale translational repressor required for
675 normal P granule formation in C. elegans. *J Cell Sci* **126**, 850-9 (2013).
676 38. Cauchi, R.J. SMN and Gemins: 'we are family' ... or are we?: insights into the
677 partnership between Gemins and the spinal muscular atrophy disease protein SMN.
678 *Bioessays* **32**, 1077-89 (2010).
679 39. Mader, S., Lee, H., Pause, A. & Sonenberg, N. The translation initiation factor eIF-4E
680 binds to a common motif shared by the translation factor eIF-4 gamma and the
681 translational repressors 4E-binding proteins. *Mol Cell Biol* **15**, 4990-7 (1995).
682 40. Gruner, S. et al. The Structures of eIF4E-eIF4G Complexes Reveal an Extended
683 Interface to Regulate Translation Initiation. *Mol Cell* **64**, 467-479 (2016).
684 41. Minasaki, R., Puoti, A. & Streit, A. The DEAD-box protein MEL-46 is required in the
685 germ line of the nematode Caenorhabditis elegans. *BMC Dev Biol* **9**, 35 (2009).
686 42. Keiper, B.D. et al. Functional characterization of five eIF4E isoforms in Caenorhabditis
687 elegans. *J Biol Chem* **275**, 10590-6 (2000).

688 43. Maris, C., Dominguez, C. & Allain, F.H. The RNA recognition motif, a plastic RNA-
689 binding platform to regulate post-transcriptional gene expression. *FEBS J* **272**, 2118-
690 31 (2005).
691 44. Schirle, N.T. & MacRae, I.J. The crystal structure of human Argonaute2. *Science* **336**,
692 1037-40 (2012).
693 45. Siomi, M.C., Mannen, T. & Siomi, H. How does the royal family of Tudor rule the
694 PIWI-interacting RNA pathway? *Genes Dev* **24**, 636-46 (2010).
695 46. Philippe, L. et al. An in vivo genetic screen for genes involved in spliced leader trans-
696 splicing indicates a crucial role for continuous de novo spliced leader RNP assembly.
697 *Nucleic Acids Res* **45**, 8474-8483 (2017).
698 47. Xu, C. et al. Structural insights into Gemin5-guided selection of pre-snRNAs for snRNP
699 assembly. *Genes Dev* **30**, 2376-2390 (2016).
700 48. Zanetti, S., Meola, M., Bochud, A. & Puoti, A. Role of the C. elegans U2 snRNP protein
701 MOG-2 in sex determination, meiosis, and splice site selection. *Dev Biol* **354**, 232-41
702 (2011).
703 49. Ferguson, K.C., Heid, P.J. & Rothman, J.H. The SL1 trans-spliced leader RNA performs
704 an essential embryonic function in Caenorhabditis elegans that can also be supplied
705 by SL2 RNA. *Genes Dev* **10**, 1543-56 (1996).
706 50. Edgar, R.C. MUSCLE: multiple sequence alignment with high accuracy and high
707 throughput. *Nucleic Acids Res* **32**, 1792-7 (2004).
708 51. Robert, X. & Gouet, P. Deciphering key features in protein structures with the new
709 ENDscript server. *Nucleic Acids Res* **42**, W320-4 (2014).
710

Gene	Allele	Mutation Type	21U RNA Presence	Terminal Phenotypes	Ratio (%)
ife-3	*xf101*	Start Codon Loss	n.d.	Mog/Mel	n.d.
	xf102	Frameshift	-	Mog/Mel	n.d.
	RNAi	n.a.	n.d.	Mog/Mel	47/53#
pid-3	*tm2417*	Frameshift	--	Mel	100
	xf149	Frameshift	n.d.	Mel	100
	xf151	Inframe Deletion	n.d.	Mel	100
	xf153	Frameshift	n.d.	Mel	100
tofu-6	*it20*	Nonsense	n.d.	Mel	100
	yt2	Nonsense	n.d.	Mel	100
	RNAi	n.a.	--*	Mel	n.d.
tost-1	*xf191*	Frameshift	n.d.	Viable	n.d.
	xf194	Start Codon Loss	+	Mel	100
	xf196	Splice Site Loss	n.d.	(TS) Mel	100 (25°C)
pid-1	*xf14*	Missense	--	n.d.	n.d.
	xf35	Frameshift	--	Mog	<1
	xf36	Frameshift	--	n.d.	n.d.
erh-2	*xf168*	Stop Codon Loss	--	Mel	100

Figure 1

a

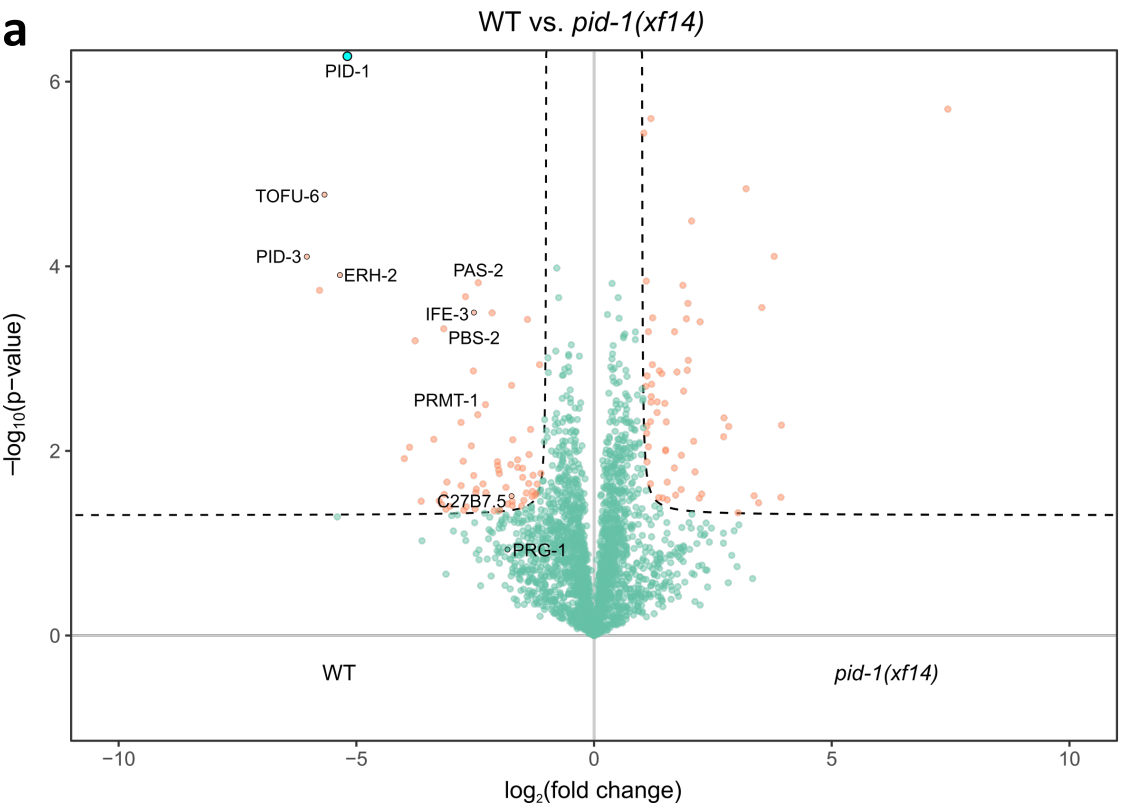
WT vs. pid-1(xf14)
PID-1
TOFU-6
PID-3
ERH-2
PAS-2
IFE-3
PBS-2
PRMT-1
C27B7.5
PRG-1
WT
pid-1(xf14)
−log10(p−value)
log2(fold change)
6
4
2
0
−10
−5
0
5
10

b

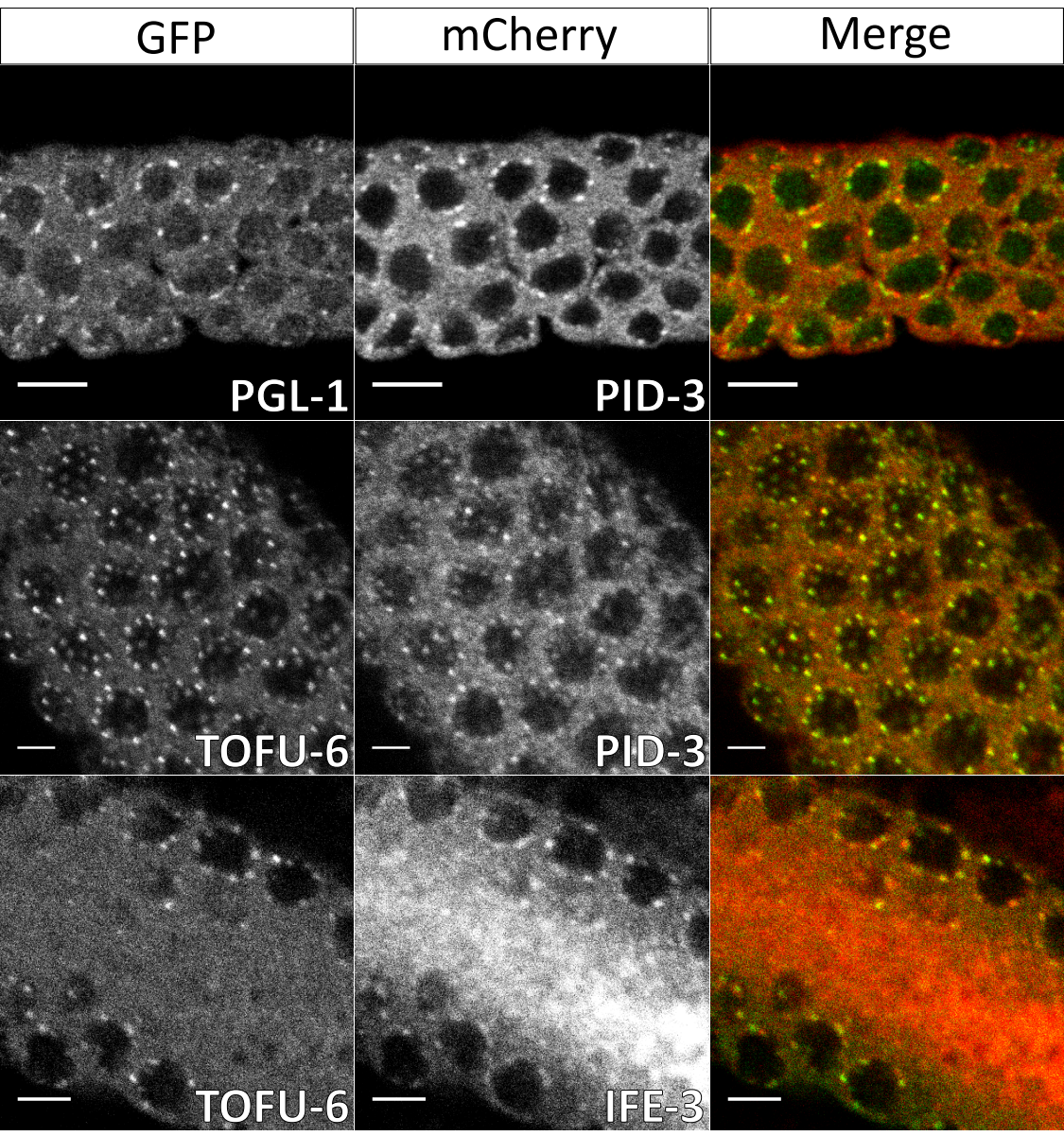
GFP
mCherry
Merge
PGL-1
PID-3
TOFU-6
PID-3
TOFU-6
IFE-3

c

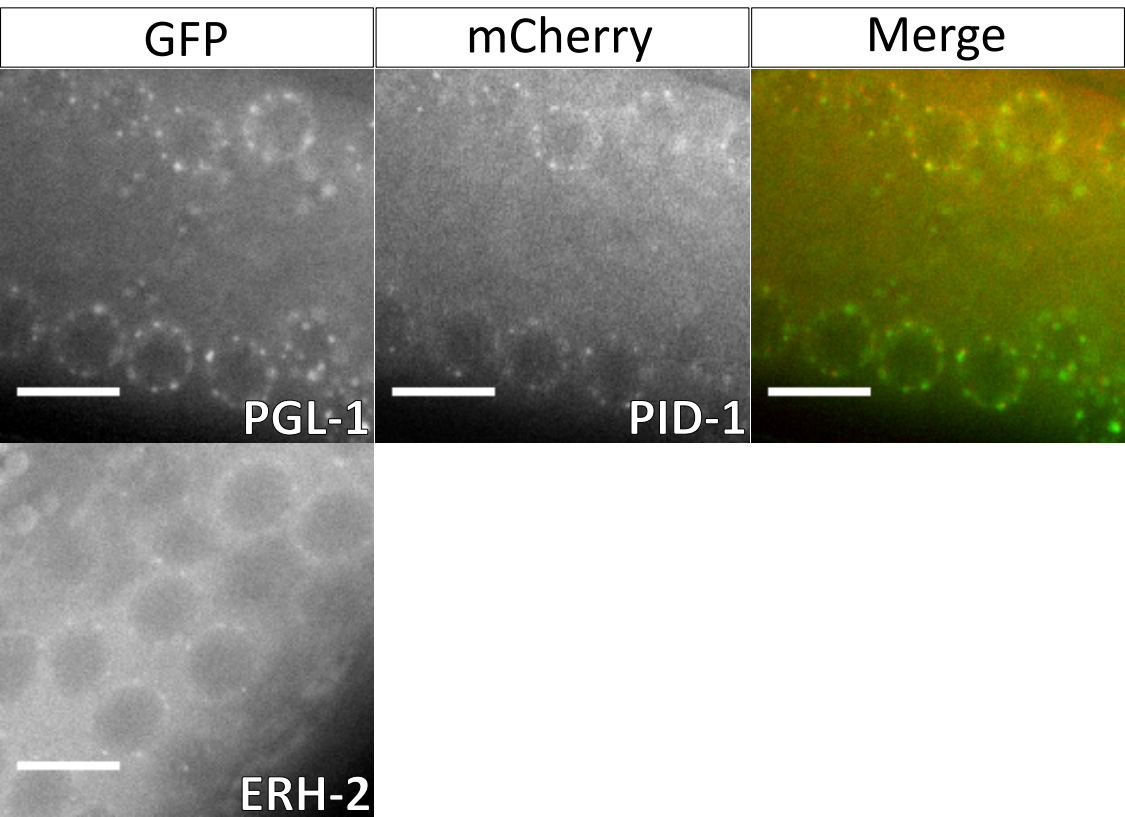
GFP
mCherry
Merge
PGL-1
PID-1
ERH-2

Figure 2

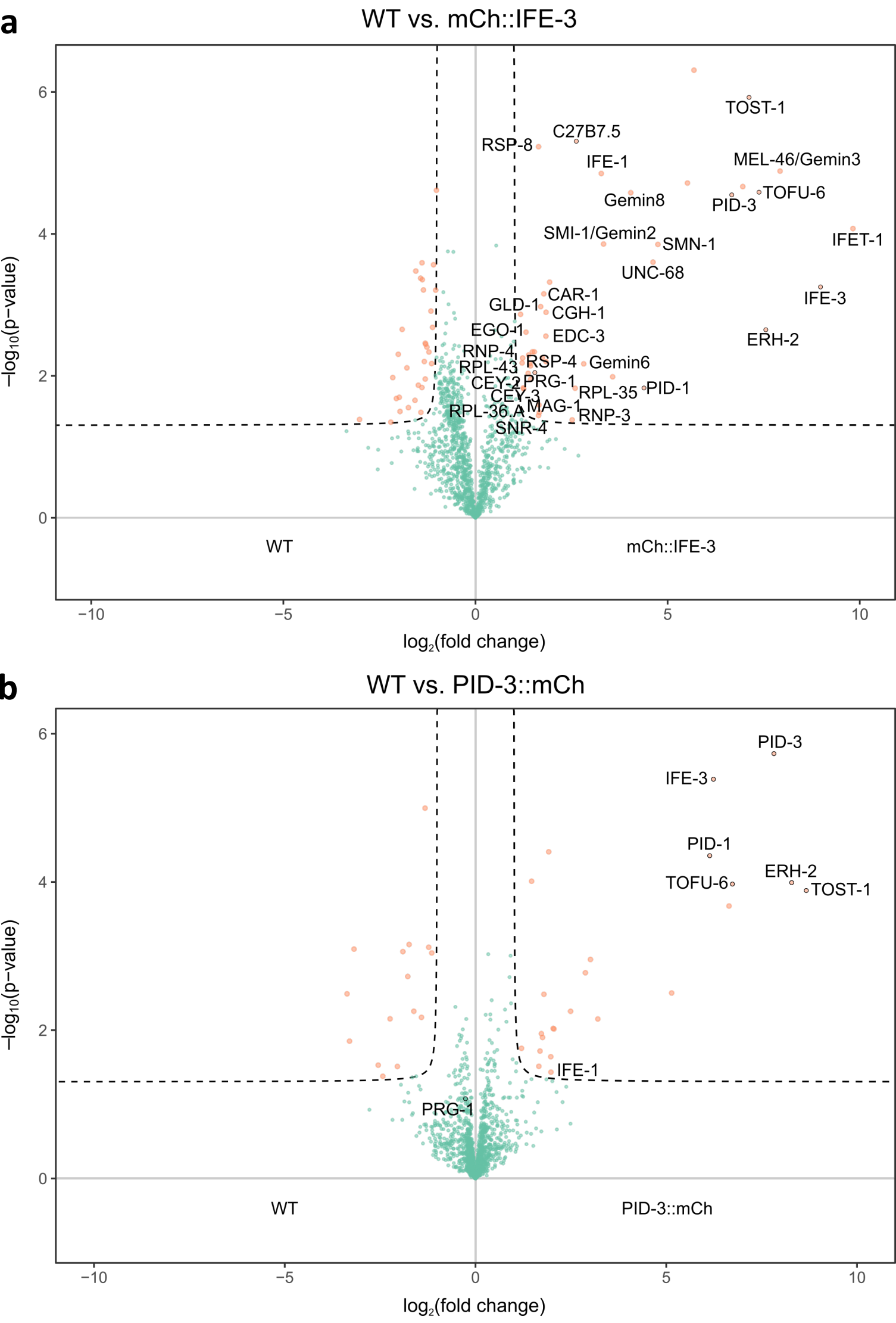
a
WT vs. mCh::IFE-3
TOST-1
C27B7.5
RSP-8
IFE-1
MEL-46/Gemin3
TOFU-6
Gemin8
PID-3
SMI-1/Gemin2
SMN-1
IFET-1
UNC-68
CAR-1
GLD-1
CGH-1
IFE-3
EGO-1
EDC-3
ERH-2
RNP-4
RPL-43
RSP-4
Gemin6
CEY-2
PRG-1
CEY-3
RPL-35
PID-1
RPL-36.A
MAG-1
RNP-3
SNR-4
WT
mCh::IFE-3
−10
−5
0
5
10
log2(fold change)
−log10(p−value)
b
WT vs. PID-3::mCh
PID-3
IFE-3
PID-1
ERH-2
TOFU-6
TOST-1
IFE-1
PRG-1
WT
PID-3::mCh
log2(fold change)
−log10(p−value)
c
WT vs. TOFU-6::GFP
PID-3
TOST-1
IFE-3
TOFU-6
IFE-1
ERH-2
C27B7.5
GLD-1
PID-1
WT
TOFU-6::GFP
log2(fold change)
−log10(p−value)
d
WT vs. ERH-2::GFP
IFE-3
ERH-2
TOST-1
TOFU-6
PID-3
T17H7.1
WT
ERH-2::GFP
log2(fold change)
−log10(p−value)
e
IFE-3 IP
SMN-1
Gemin3
RPL-36.A
RNP-3
Gemin2*
Gemin6*
UNC-68
Gemin8
IFET-1
T14G10.8
C44B9.2
T21B10.3*
TOFU-6 IP
IFE-1
C27B7.5*
F55G1.9
F38B2.4
T17H7.1
Y54F10AM.6
C34G6.6
C06A8.3
ERH-2 IP
IFE-3
TOFU-6
PID-3
ERH-2
TOST-1
PID-1
PID-3 IP
Y41C4A.32
PAS-2
PBS-2
PRMT-1
GLDC-1
PID-1 IP

Figure 3

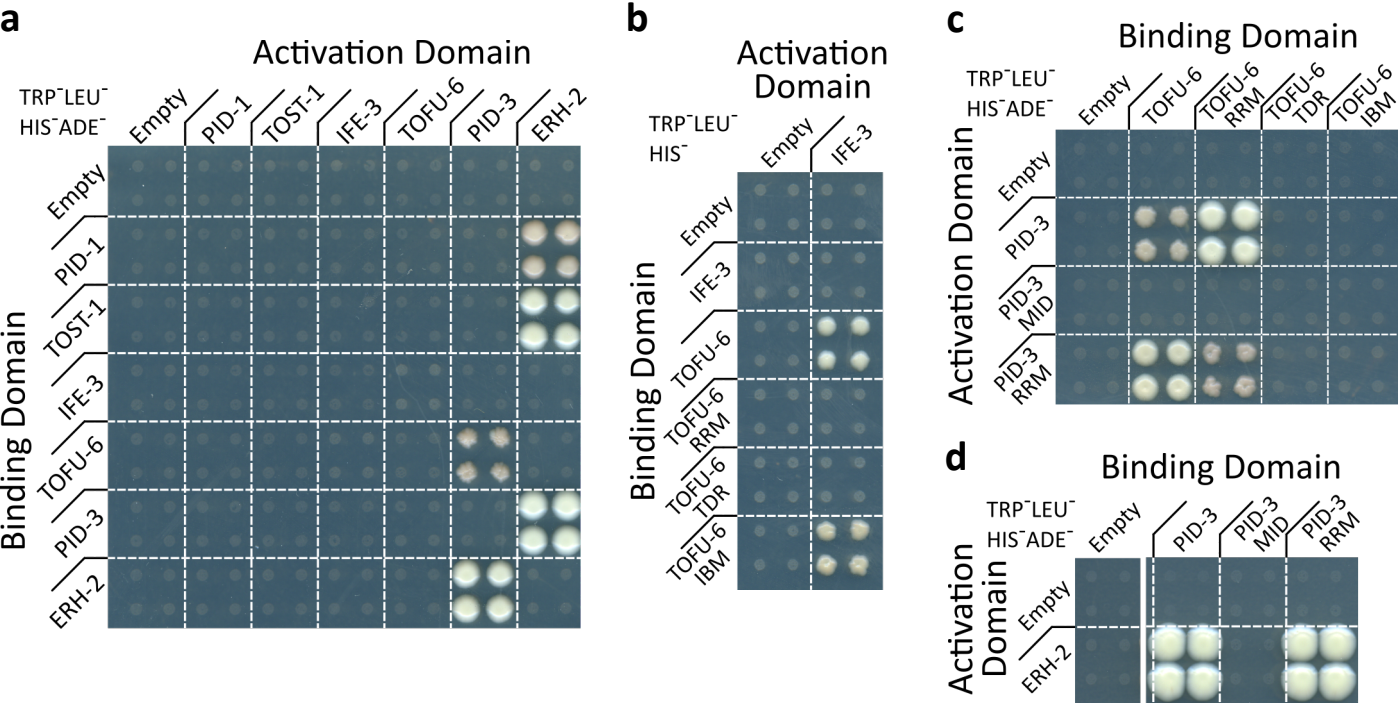
a
Activation Domain
TRP⁻LEU⁻
HIS⁻ADE⁻
Empty
PID-1
TOST-1
IFE-3
TOFU-6
PID-3
ERH-2
Binding Domain
b
Activation Domain
TRP⁻LEU⁻
HIS⁻
Empty
IFE-3
Binding Domain
TOFU-6
TOFU-6 RRM
TOFU-6 TDR
TOFU-6 IBM
c
Binding Domain
TRP⁻LEU⁻
HIS⁻ADE⁻
Empty
TOFU-6
TOFU-6 RRM
TOFU-6 TDR
TOFU-6 IBM
Activation Domain
PID-3
PID-3 MID
PID-3 RRM
d
Binding Domain
TRP⁻LEU⁻
HIS⁻ADE⁻
Empty
PID-3
PID-3 MID
PID-3 RRM
Activation Domain
ERH-2

Figure 4

a

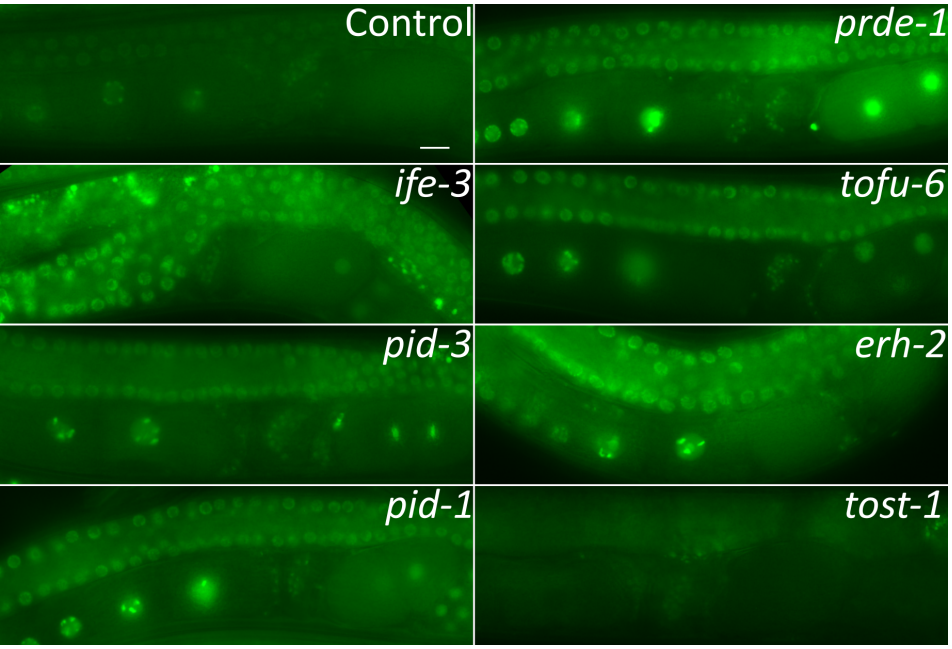
Control
prde-1
ife-3
tofu-6
pid-3
erh-2
pid-1
tost-1

b

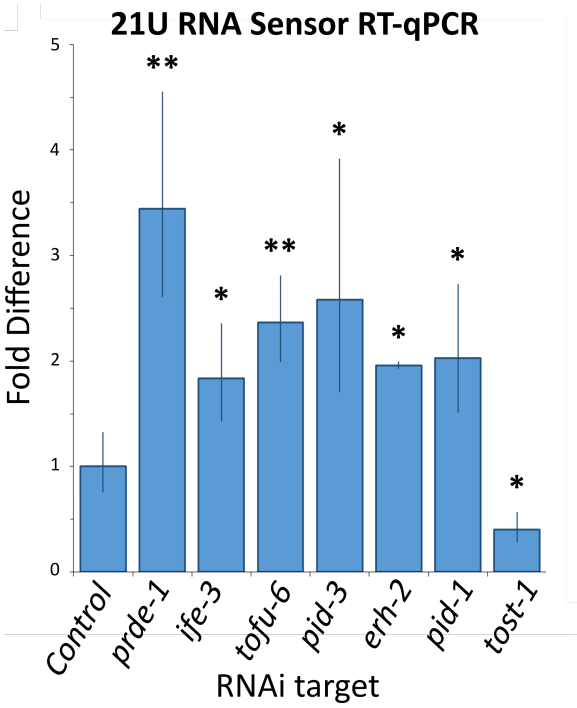
21U RNA Sensor RT-qPCR
Fold Difference
0
1
2
3
4
5
**
*
**
*
*
*
*
Control
prde-1
ife-3
tofu-6
pid-3
erh-2
pid-1
tost-1
RNAi target

c

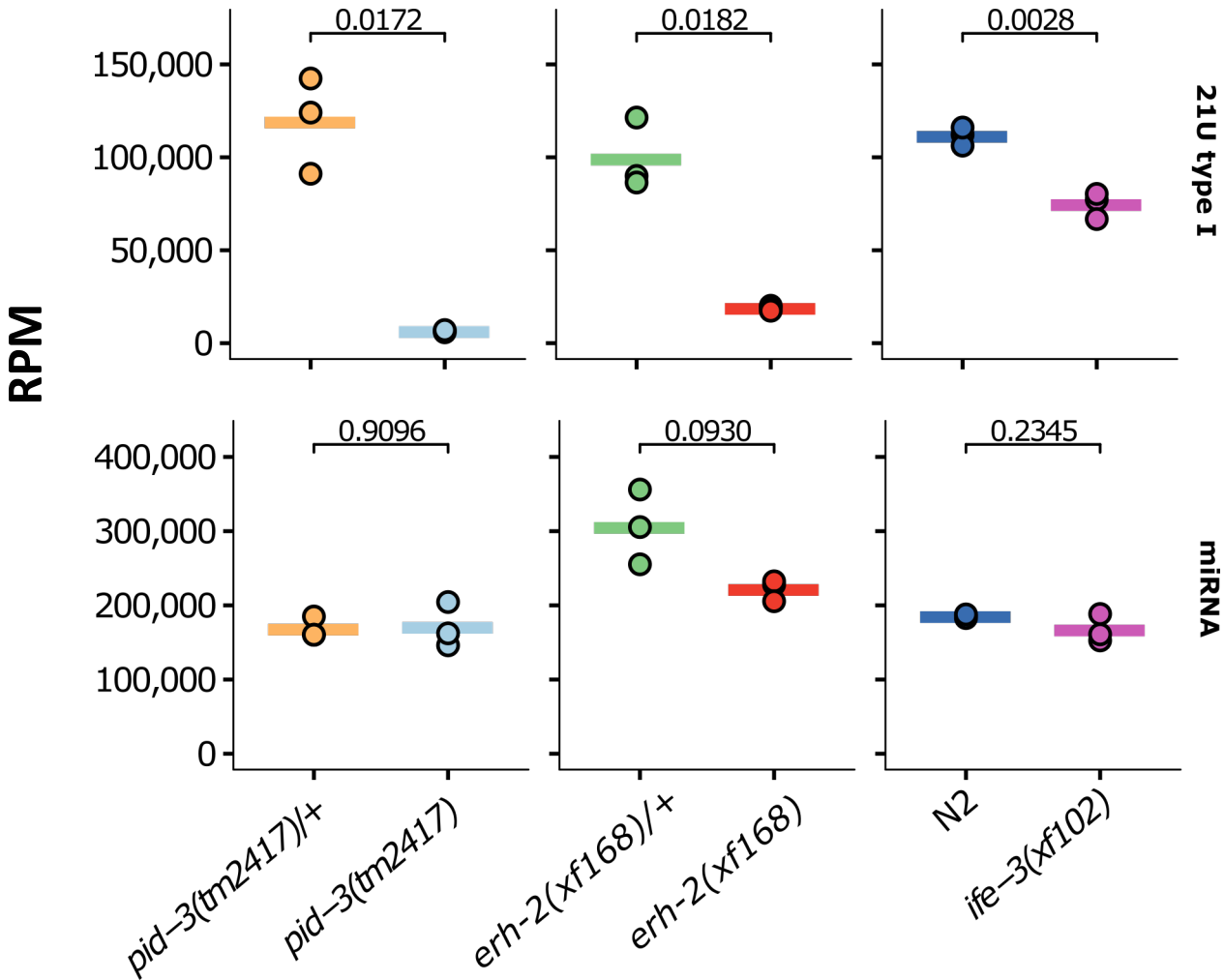
RPM
0.0172
0.0182
0.0028
150,000
100,000
50,000
0
21U type I
0.9096
0.0930
0.2345
400,000
300,000
200,000
100,000
0
miRNA
pid-3(tm2417)/+
pid-3(tm2417)
erh-2(xf168)/+
erh-2(xf168)
N2
ife-3(xf102)

Figure 5

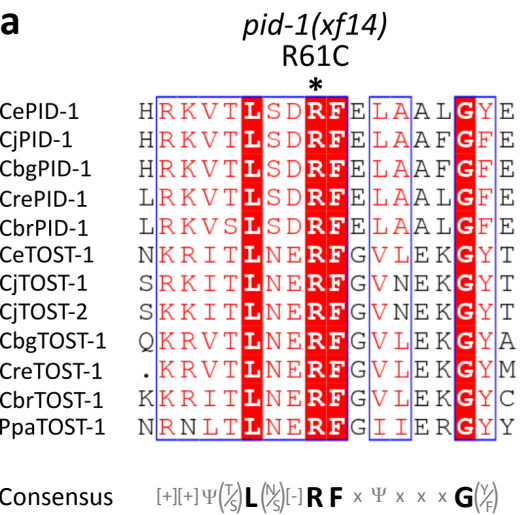
a
pid-1(xf14)
R61C
*
CePID-1 HRKVTLSDRFELAALGYE
CjPID-1 HRKVTLSDRFELAAFGFE
CbgPID-1 HRKVTLSDRFELAAFGFE
CrePID-1 LRKVTLSDRFELAALGFE
CbrPID-1 LRKVSLSDRFELAALGFE
CeTOST-1 NKRITLNERFGVLEKGYT
CjTOST-1 SRKITLNERFGVNEKGYT
CjTOST-1 SKKITLNERFGVNEKGYT
CbgTOST-1 QKRVTLNERFGVLEKGYA
CreTOST-1 .KRVTLNERFGVLEKGYM
CbrTOST-1 KKRITLNERFGVLEKGYC
PpaTOST-1 NRNLTLNERFGIIERGYY
Consensus [+][+]Ψ(T/S)L(N/S)[-]R F x Ψ x x x G(Y/F)

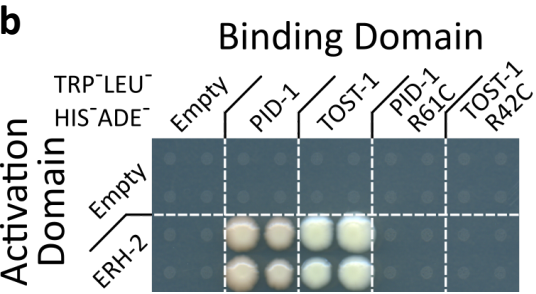
b
Binding Domain
TRP⁻LEU⁻
HIS⁻ADE⁻
Empty
PID-1
TOST-1
PID-1 R61C
TOST-1 R42C
Activation Domain
Empty
ERH-2

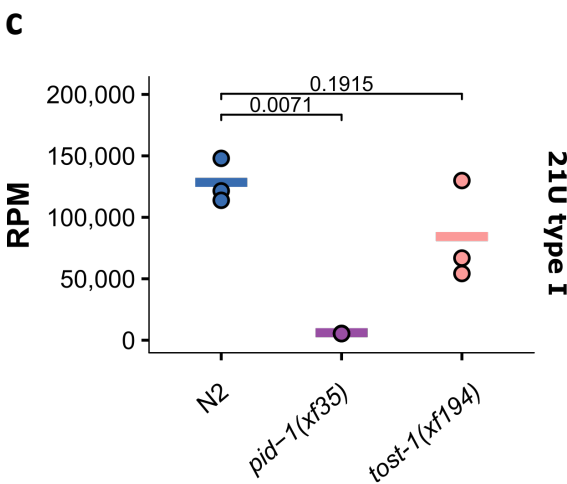
c
RPM
200,000
150,000
100,000
50,000
0
0.1915
0.0071
N2
pid−1(xf35)
tost-1(xf194)
21U type I

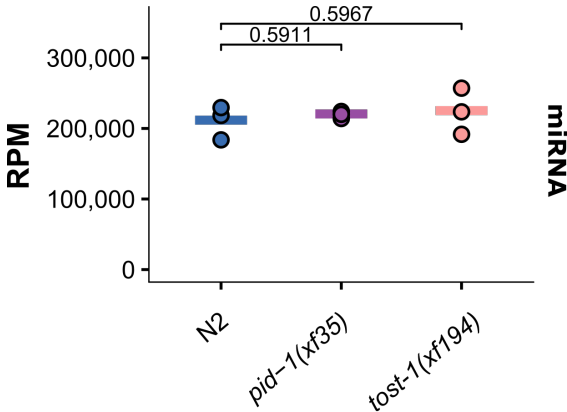
RPM
300,000
200,000
100,000
0
0.5967
0.5911
N2
pid−1(xf35)
tost-1(xf194)
miRNA

Figure 6

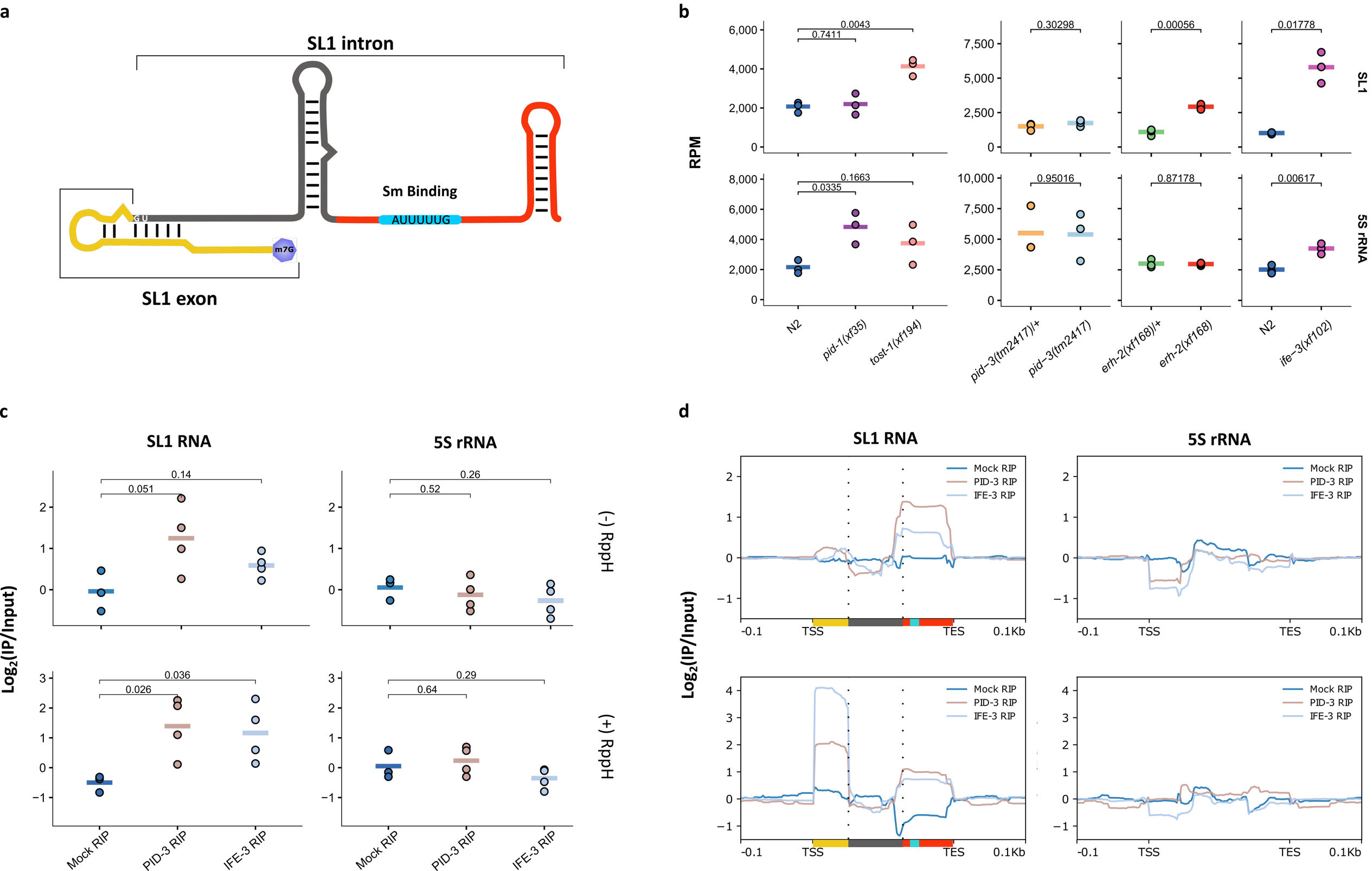
a
SL1 intron
Sm Binding
AUUUUUG
m7G
SL1 exon
b
RPM
SL1
5S rRNA
0.0043
0.7411
0.30298
0.00056
0.01778
0.1663
0.0335
0.95016
0.87178
0.00617
N2
pid-1(xf35)
tost-1(xf194)
pid-3(tm2417)/+
pid-3(tm2417)
erh-2(xf168)/+
erh-2(xf168)
N2
ife-3(xf102)
c
SL1 RNA
5S rRNA
Log2(IP/Input)
(-) RppH
(+) RppH
0.14
0.051
0.26
0.52
0.036
0.026
0.29
0.64
Mock RIP
PID-3 RIP
IFE-3 RIP
d
SL1 RNA
5S rRNA
Log2(IP/Input)
(-) RppH
(+) RppH
Mock RIP
PID-3 RIP
IFE-3 RIP
-0.1
TSS
TES
0.1Kb

Figure 7

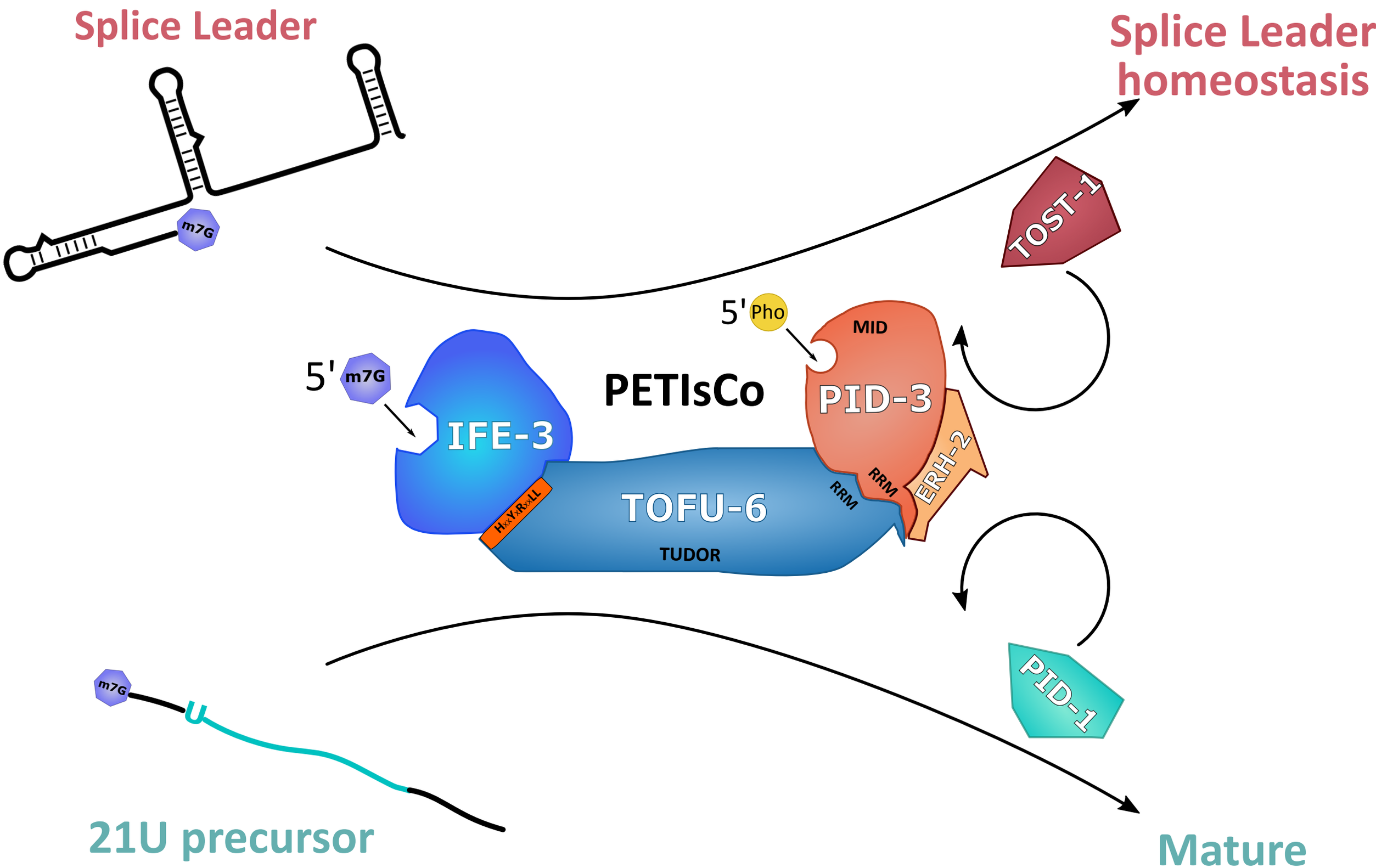
Splice Leader
m7G
Splice Leader homeostasis
TOST-1
5' Pho
MID
5' m7G
PETIsCo
PID-3
IFE-3
ERH-2
RRM
HxxYxRxxLL
TOFU-6
RRM
TUDOR
PID-1
m7G
U
21U precursor
Mature 21U RNA